

## Chapter 2

# Piezoelectric Ceramic Materials

Piezoelectric ceramic materials are polycrystals built from tiny grains (typically 1–10  $\mu\text{m}$  big), which are macroscopically homogeneous. Origin of the grains, their shapes, size distribution, and their arrangement in the texture are substantial for the resulting macroscopic material properties. Symmetry of the grain texture is defined by the symmetry of grains and by the symmetry of their mutual arrangement.

The microscopic symmetry is fully given by the material crystallographic symmetry. The effective macroscopic symmetry reflects also the information about the grains arrangement and about the finite size of the whole sample. Piezoelectricity is possible for three limiting group symmetry classes —  $\infty$ ,  $\infty m$ , and  $\infty 2$  — which do not have center of symmetry.

Ceramic materials exhibiting isotropic grains are also typical materials with isotropic properties at the macroscopic scale. This however does not allow any piezoelectric activity, while the anisotropy is needed for that. There are two possibilities how to create anisotropy in polycrystal built from grains, required for the piezoelectricity:

- Grain size and shape texture;
- Dipole moment alignment.

Grain size and shape texture might appear during grain growth for the materials with low crystallographic symmetry and preferred grain growth orientation. Such grains might exhibit whiskers-like, platelet-like, or other anisotropic shape, which results in their alignment during pressing ceramic body. Platelet-like grains are preferentially aligned in plane perpendicular to the mechanical press direction, aligned mechanically, etc. Grain size and texture is basically a possibility to create piezoelectric properties in ceramics from piezoelectric (and not ferroelectric) material with strongly piezoelectric grains and their anisotropic shape. However, this is not the case for most materials. The most ceramic materials are macroscopically isotropic with negligible piezoelectric coefficient due to random orientation of grains.

The second method, how to impose anisotropy, is based on ferroelectricity and the possible coexistence of several energetically equivalent domain states (multidomain structure), each exhibiting a unique direction of the dipole moment and related piezoelectric tensor anisotropy. Such dipole moments could be aligned at elevated temperature using strong electric field (poling). It results in the preference of certain domain states and ensures the macroscopic anisotropy of material. Poling field must be higher than coercive field in order to get stable material properties. Some materials have the dipole moments “frozen” in the structure and therefore, the higher poling temperature allows easier domain wall mobility and poling. Poling temperature should not exceed Curie temperature ( $T_C$ ), which is a limit for the dipole moment existence and ferroelectricity. Poling also results in domain wall movements and in the grain deformation. While the grains are mutually mechanically clamped in ceramic system, the macroscopic cracks could be created during harsh poling procedure.

The best effect might be expected from the combination of both methods, i.e., poling of ferroelectric ceramics with grain texture. Messing et al. (2004) reviewed technology of textured ceramics and found piezoelectric coefficient  $d_{33}$  enhancement due to texture in various ceramic materials. The best enhancement was reached for highly textured ceramics of bismuth layer structure compound (e.g.,  $\text{Sr}_{0.3}\text{Bi}_{3.7}\text{Ti}_{2.7}\text{Ta}_{0.3}\text{O}_{12}$  with 3.4 times higher  $d_{33}$  coefficient than for non-textured polycrystal, tungsten bronze family up to 2–3 times higher  $d_{33}$  for  $\text{Sr}_{0.53}\text{Ba}_{0.47}\text{Nb}_2\text{O}_6$  and up to 2.1 times higher in perovskite family).

Poled piezoelectric ceramics exhibit macroscopic  $\infty m$  symmetry, which is characterized by 10 independent electromechanical material coefficients (5 elastic, 3 piezoelectric, and 2 dielectric). This symmetry is the same no matter what is the symmetry of the ceramic grain material. Mostly the perovskite ferroelectric materials with tetragonal  $4mm$  (e.g.,  $\text{BaTiO}_3$  and  $\text{PbTiO}_3$ ), rhombohedral  $3m$  (e.g., PMN-PT), or orthorhombic  $mm2$  (e.g.,  $\text{KNbO}_3$  and  $\text{NaNbO}_3$ ) symmetry are used in making piezoelectric ceramics. Intergranular stresses are minimized by the formation of domains. Number of permissible domain states depends on the ferroelectric species. Assuming the random grain orientations and complete dipole alignment, the ratios of ceramic versus single-crystal spontaneous polarizations allowed for different perovskite species were calculated by Redin et al. (1963) — see Table 2.1.

Isotropy of piezoelectric ceramics is destroyed during poling process but remains in the direction perpendicular to the poling field direction; i.e., poling direction is  $\infty$ -fold axis of symmetry. Structure of tensor material coefficients for the limiting

**Table 2.1** Net polarization in ceramics allowed by symmetry as a ratio of the single-crystal spontaneous polarization (Redin et al. 1963)

Ferroelectric species	Number of permissible domain states	$P_S$ orientation [parent phase coordinates]	$\bar{P}_S/P_S$
$m\bar{3}m \rightarrow 4mm$	6	$\langle 100 \rangle$	0.831
$m\bar{3}m \rightarrow 3m$	8	$\langle 111 \rangle$	0.866
$m\bar{3}m \rightarrow mm2$	12	$\langle 110 \rangle$	0.912

$\infty m$  polar symmetry is the same as for the hexagonal  $6mm$  symmetry for dielectric, piezoelectric, and elastic tensors.

The main advantages of piezoelectric ceramics include:

- Low cost compared to single-crystalline material form
- Possibility of complex shaping (plates, disks, tubes, focal bowls, etc.)
- Possibility to prepare ceramics even if crystals are not successfully grown (e.g., PZT).

However, there are also some factors, which limit piezoelectric ceramics application:

- Worse material reproducibility due to polycrystalline form with complex ceramic processes involved during ceramics processing
- Loss of piezoelectricity above Curie temperature and practical temperature limit smaller than this temperature
- Higher temperature coefficients of material properties
- Higher electrical conductivity than single-crystalline material
- Pyroelectricity related to ferroelectricity of material (but it might be also advantageous property for pyroelectric applications).

The chemical composition of piezoelectric ceramics may include all ferroelectric compounds, but the most successful structures ever belong to the perovskite crystallographic structure, solid solutions of perovskites, bismuth layer compounds, and tungsten bronze structures.

First system of piezoelectric ceramics ( $\text{BaTiO}_3$ ) has been developed at the end of World War II independently in Japan, Soviet Union, and USA. Ceramic material was used for the applications in ultrasonic (electroacoustic) transducers. Later in the 1950s, the most important ceramic system ever — solid solutions of  $\text{PbZrO}_3$ – $\text{PbTiO}_3$  (PZT) — was investigated. It is the mostly used piezoelectric ceramics in today's applications. Since that time many new ceramic compositions (oxides, complex perovskites, and relaxors) are under intensive research. The last two decades were devoted to very intense study of lead-free materials due to environmental issues. Although the lead-free materials research resulted in the materials with properties approaching PZT material properties, it is not yet in larger commercial application today (Sonox® P1 LF from CeramTec Company could serve as an example of lead-free commercially available material).

## 2.1 PZT Ceramics

Piezoelectric ceramic materials based on the solid solutions of  $\text{PbZrO}_3$  (PZ) and  $\text{PbTiO}_3$  (PT) — known as PZT ceramics — have been studied, applied, and manufactured already for 60 years (Jaffe et al. 1971; Berlincourt 1981; Setter and Colla 1993; Buchanan 1986; Levinson 1988; Nowotny 1992; Bhalla et al. 2000;

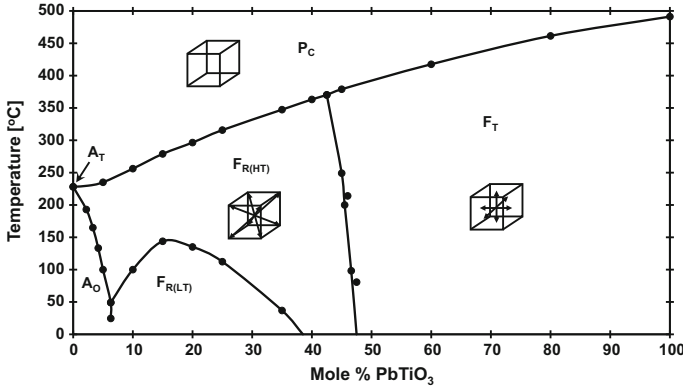


**Fig. 2.1** Phase diagram of PZT solid solution system, according to Jaffe et al. (1971)

Cross 1996; Heywang et al. 2008). It has excellent piezoelectric properties, which could be designed to meet specific application needs by the doping. Due to large-scale commercial production, PZT ceramics is available at reasonable prices for many applications in bulk form. Its multilayer form is however much more expensive because of large amount of noble metals used for electrodes.

PZT solid solution exhibits the morphotropic phase boundary (MPB) at 48–52 % PT content in the temperature range important for technical applications (for phase diagram, see Fig. 2.1). Basic unit of PZT is the perovskite structure with Pb atoms at  $A^{2+}$  positions and alternating Zr and Ti atoms at  $B^{4+}$  positions at the ratio given by the solid solution composition (Fig. 2.2).

Paraelectric solid phase exists above Curie temperature and ferroelectric phases below Curie temperature. Pure PT is tetragonal ferroelectric ( $4mm$ ), and pure PZ is antiferroelectric with orthorhombic structure at room temperature. MPB is a boundary between tetragonal ( $4mm$ ) and rhombohedral ( $3m$ ) ferroelectric phases. Paraelectric phase exhibits cubic  $m\bar{3}m$  symmetry. The MPB is a composition region of PZT ceramics with the same structure of coexistence of two phases with 6

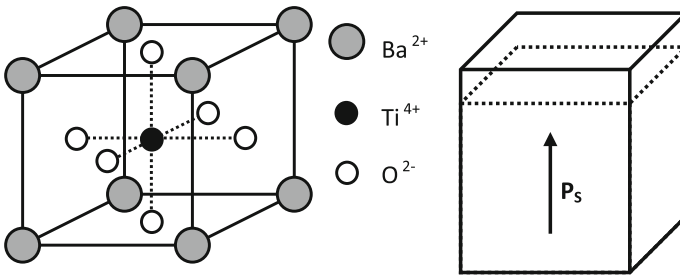


**Fig. 2.2** Basic unit of perovskite structure of  $BaTiO_3$  and spontaneous polarization direction in tetragonal phase, according to Tichý et al. (2010)

**Table 2.2** Applicability limits for electric field and mechanical stress for selected PZT ceramics (PXE® is the registered trademark of Philips)

Material grade	$E_{\max}$ [Vmm <sup>-1</sup> ]	$T_{\max}$ [MPa]
PXE 59	350	5
PXE 5	300	2.5
PXE 52	100	–
PXE 41	300	10
PXE 42	400	25
PXE 43	500	35

domain states in tetragonal and 8 domain states in rhombohedral ferroelectric phase. Maximum or minimum values of material coefficients of PZT ceramics appear for the chemical composition at the rhombohedral side of MPB.

Existence of ferroelectricity is the main thermal limit for the application of PZT ceramics since the piezoelectric properties are lost above Curie temperature  $T_C$ . It is recommended by PZT manufacturers not to use PZT ceramics above  $1/2T_C$ . Curie temperatures for commercially produced PZTs are usually between 150 and 360 °C (Material data sheets of manufacturers — see Table 2.3). Another operational limit of PZT ceramics is imposed by the application of electric field, which can revert spontaneous polarization. Piezoelectric ceramics is more sensitive to the application of electric field antiparallel to the spontaneous polarization vector (typically an ac electric field), than to parallel one. Similarly to the electric field and temperature, the limits for PZT applicability exist also for the mechanical prestress. Mechanical stress imposes the preference of polarization orientation in plane perpendicular to the direction of applied mechanical stress according to Curie's law. Excessive mechanical stresses can depolarize the ceramics similarly to the electric field and temperature. Typical values for the electric field and mechanical stress limiting PZT applications are given in Table 2.2. Mechanical prestress is used in ultrasound or sensor technology to ensure good mechanical transfer of ultrasonic wave and to shift the working mechanical stress into the compression stress range. Mechanical tension could damage brittle ceramics and its excessive application in power ultrasound technology might even result in mechanical fracture of ceramics.

Material properties of PZT ceramics could be modified by the doping of small amount (up to several %) of foreign atoms. There might be additions of isovalent atoms ( $\text{Sr}^{2+}$ ,  $\text{Ca}^{2+}$ ,  $\text{Ba}^{2+}$ ) or heterovalent atoms such as donors or acceptors (Heywang et al. 2008). Specific additions of donors occupying  $\text{B}^{4+}$  positions (e.g.,  $\text{Nb}^{5+}$ ,  $\text{Sb}^{5+}$ , and  $\text{W}^{6+}$ ) or occupying  $\text{A}^{2+}$  positions (e.g.,  $\text{La}^{3+}$  and  $\text{Bi}^{3+}$ ) modify PZT ceramics to “soft” PZT with the dipole moments easily switchable. Special type of PZT ceramics is a La-doped PZT, commonly abbreviated as PLZT. Such ceramics is transparent and level of transparency could be controlled by the applied electric field. Another additions of acceptors occupying  $\text{B}^{4+}$  positions (e.g.,  $\text{Fe}^{3+}$ ,  $\text{Al}^{3+}$ ,  $\text{Ni}^{3+}$ , and  $\text{Mn}^{2+}$ ) or occupying  $\text{A}^{2+}$  positions (e.g.,  $\text{K}^{+}$  and  $\text{Ag}^{+}$ ) create “hard” PZT with the dipole moments hardly reversible. Soft and hard PZT are two main types of PZT ceramic materials. While soft materials are applied for sensoric functions due to their higher piezoelectric coefficients, hard PZT materials are suitable for power ultrasonics due to their lower mechanical losses. Chemical composition and

processing is usually not known to the end users of PZT products. For the typical properties of PZT ceramics available commercially, see Table 2.3.

PZT ceramics is produced commercially by powder metallurgy processing. Raw materials of  $\text{PbO}$ ,  $\text{ZrO}_2$ , and  $\text{TiO}_2$  are mixed in water solution in a ball mill in order to homogenize powder chemical composition. Specific doping atoms (e.g., in the form of oxide  $\text{Nb}_2\text{O}_5$ , carbonate, or other) are added and mixed together with basic oxides. Subsequently drying and sintering processes take place. Crystallographic water is released from raw materials in this process. The chemical reaction to the solid solution is finished. Material is milled again to the powder with the grains of typical size 1–10  $\mu\text{m}$  and an organic binder is added. Raw material is now ready for the forming to the “green body” (either by mechanical press or by tape-casting). PZT elements are subsequently heated in order to fire out organic binder polymer. Due to the binder addition to the ceramic material, pores of certain size are necessarily present in the ceramic body. Then the piezoelectric element is ready for mechanical shaping (cutting, lapping, and polishing, etc., by the diamond tools). After the shaping, PZT elements are covered by electrode either by Ag-paste screen plating (and electrode firing) or by Au-sputtering. Electrical poling and material property testing are the final manufacturing operations. Poling is done in oil bath at higher temperature with subsequent chemical and ultrasonic cleaning. Typical values of the poling field are 2–4 kV/mm and differ for the soft and hard PZT types. Hard PZT ceramics gets higher electric conductivity at higher temperatures. An optimum poling condition must be found as a compromise between PZT conductivity, poling field, and temperature. Another possibility to pole PZT ceramics is so-called field cooling method. PZT ceramics is heated to the temperature above the Curie temperature, small electric field (e.g., 100 V/mm) is applied, and sample is slowly cooled down to room temperature. Such technique however needs much time and therefore, it is not commercially used in PZT production. Piezoelectric coefficient, resonance frequency, capacity, etc., are measured and elements are 100 % tested by PZT manufacturers. Commercial reproducibility in material parameters for each batch of raw powder however cannot be fully met in ceramic materials.

Domain structure is the main reason for the hysteretic behavior of PZT ceramics. In D-E diagram, the typical shape of hysteresis loop is observed (see Fig. 2.3). Typical values of the coercive field are 0.5–2 kV/mm and spontaneous polarization is 20–30  $\mu\text{C}/\text{cm}^2$  for different PZT types. Area of hysteresis loop represents volume density of heat dissipated within the material during one cycle of domain switching. Domain walls are easily movable in soft PZT ceramics and hysteresis losses are higher (order of magnitude 1 %). More difficult mobility of domain walls is a reason for smaller dielectric losses (order of magnitude 0.1 %) in hard PZT. Due to the piezoelectric effect, hysteresis loop is observed also for the elastic strain  $S$  as a function of electric field  $E$  (S-E loop, so-called butterfly loop).

**Table 2.3** Material data for selected piezoelectric ceramics available commercially

Property	Soft PZT					Hard PZT				
	Pz29	NCE51	SONOX P502	PZT5H2	APC850	Pz24	NCE40	SONOX P8	PZT802	APC841
$s_{11}^E$	17.0	17.0	18.5	16.4	15.9	10.5	13.0	11.4	11.5	13.2
$s_{12}^E$	-5.78	-5.36	-	-	-	-3.13	-	-	-	-
$s_{13}^E$	-8.79	-8.69	-	-	-	-4.77	-	-	-	-
$s_{33}^E$	22.9	21.3	20.7	20.8	18.5	13.6	17.0	13.7	13.5	15.9
$s_{44}^E$	54.1	48.9	-	-	-	32.4	-	-	-	-
$\epsilon_{11}^T$	2440	1940	1950	-	-	739	-	1250	1290	-
$\epsilon_{33}^T$	2870	1900	1850	3400	1900	425	1250	1000	1150	1375
$k_p$	64.3	65	62	65	63	49.4	58	55	54	60
$k_t$	52.4	50	48	-	-	50.8	50	48	-	-
$k_{31}$	37.0	38	33	39	36	29.2	34	30	30	33
$k_{33}$	75.2	74	72	75	72	65.9	70	68	64	68
$k_{15}$	67.1	73	74	68	68	53.7	-	60	55	67
$d_{31}$	-243	-208	-185	-274	-175	-58	-140	-95	-97	-109
$d_{33}$	574	443	440	593	400	149	320	240	250	300
$d_{15}$	724	669	560	741	590	247	-	380	300	450
$d_h$	88.2	-	-	45	-	33.4	-	-	31	-
$T_C$	235	360	335	195	360	330	318	305	300	320
$\rho$	7460	7850	7740	7450	7600	7700	7750	7700	7500	7600
$\tan \delta$	1.6	1.5	1.25	2.5	2.0	0.2	0.25	0.2	0.3	0.4
$Q_m$	76	80	80	65	80	1700	700	1000	1000	1400

Pz24 and Pz29 are the trademarks of Ferroperm Piezoceramics A/S (Denmark); NCE51 and NCE40 are the trademarks of Noliac Ceramics (Czech Republic); SONOX<sup>®</sup>P502 and SONOX<sup>®</sup>P8 are the trademarks of CeramTec (Germany); PZT5H2 and PZT802 are the trademarks of Morgan Electro Ceramics, Ltd. (UK); APC841 and APC850 are the trademarks of APC International, Ltd. (USA)

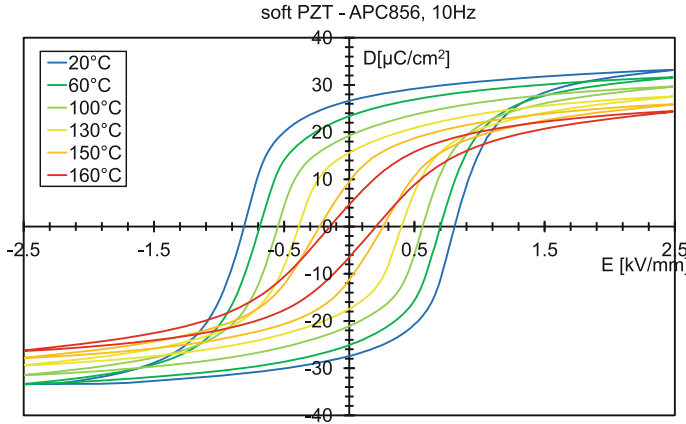


**Fig. 2.3** Temperature evolution of hysteresis loop for soft PZT ceramics, type APC856 (APC International, Ltd., USA)

## 2.2 Other Ceramic Compositions

Other piezoelectric ceramic materials are specially designed in order to improve material properties of PZT system — mainly in Curie temperature, mechanical coupling, and also to meet environmental issues (lead-free materials). PZT ceramics exhibits relatively small Curie temperature and therefore, it could be applied only within lower temperature range. There are several ceramic systems, which are commercially available and used in applications mainly for their high Curie temperature. Other materials have no lead content and they are developed to replace PZT ceramics once they achieve similar material parameters.

Non-PZT materials belong to several structural classes (for material properties, see Table 2.4):

- Perovskites, e.g.,  $\text{BaTiO}_3$ , are lead-free ceramic materials. Its application is limited by the structural phase transitions within technical temperature range (phase transition from tetragonal to orthorhombic ferroelectric phase at 5 °C) and by relatively low Curie temperature (only about 120 °C). Another perovskite is tetragonal  $\text{PbTiO}_3$  ceramics doped with Ca atoms ( $T_C = 490$  °C), and it exhibits also high hydrostatic piezoelectric coefficient. Many lead-free ceramic compositions based on perovskite structure are studied (for more details, see, e.g., Priya and Nahm 2012; Shrout and Zhang 2007; Rödel et al. 2015):
  - $\text{KNbO}_3\text{--NaNbO}_3$  (KNN) system (Saito et al. 2004) doped with various additional atoms such as solid solutions with  $\text{LiNbO}_3$ ,  $\text{LiTaO}_3$ ,  $\text{LiSbO}_3$ , etc. Doping is studied in order to design phase transition temperatures with keeping reasonable values of piezoelectric properties at the same time. This system however faces difficulties in obtaining fully dense samples and



**Table 2.4** Material properties of selected non-PZT ceramic materials

Property		Pz34 doped PbTiO <sub>3</sub>	Pz35 PbNb <sub>2</sub> O <sub>6</sub>	Pz46 modified Bi <sub>4</sub> Ti <sub>3</sub> O <sub>12</sub>	BaTiO <sub>3</sub> ceramics	SONOX P1 LF lead-free
$s_{11}^E$	[10 <sup>-12</sup> Pa <sup>-1</sup> ]	7.33	—	10.6	8.55	8.2
$s_{12}^E$		-1.61	—	—	-2.61	—
$s_{13}^E$		-0.536	—	—	-2.85	—
$s_{33}^E$		7.31	—	44.2	8.93	8.5
$s_{44}^E$		17.2	—	26.2	23.3	—
$\varepsilon_{11}^T$	[ $\varepsilon_0$ ]	237	247	127	—	1330
$\varepsilon_{33}^T$		208	219	124	1350 – 1700	1150
$k_p$	[%]	7.4	—	3.3	37.8	31
$k_t$		40.9	33.6	24.9	—	45
$k_{31}$		4.6	—	2.1	20.8	18
$k_{33}$		39.7	—	8.7	49.3	43
$k_{15}$		22.8	16.9	4.5	47.6	38
$d_{31}$	[pC/N]	-5.33	—	-2.26	-79	52
$d_{33}$		46.0	83.0	19.1	191	135
$d_{15}$		43.3	53.9	7.79	270	210
$d_h$		35.3	—	14.6	—	—
$T_C$	[°C]	400	500	650	130	115
$\rho$	[kgm <sup>-3</sup> ]	7550	5720	6530	—	5700
$\tan \delta$	[%]	1.4	0.6	0.4	—	0.8
$Q_m$	[-]	700	17	1700	—	310

Pz34, Pz35, and Pz46 are the trademarks of Ferroperm Piezoceramics A/S (Denmark); SONOX®P1 LF is the trademark of CeramTec (Germany)

reproducibility of properties. Addition of Cu atoms to KNN system results in high mechanical quality factor  $Q_m \approx 2500$  (Yang et al. 2013).

- (Na<sub>1/2</sub>Bi<sub>1/2</sub>)TiO<sub>3</sub> (NBT) or (K<sub>1/2</sub>Bi<sub>1/2</sub>)TiO<sub>3</sub> (KBT) in solid solutions with BaTiO<sub>3</sub> (BT), or in secondary systems with morphotropic phase boundary such as NBT-BT, KBT-BT, or in ternary system NBT-KBT-BT.
- (Ba,Ca),(Ti,Zr)O<sub>3</sub> system having high piezoelectric constants  $d_{33} \approx 1000$  pC/N, but small Curie temperature  $T_C \approx 100$  °C.
- Layered bismuth oxides — e.g., bismuth titanate Bi<sub>4</sub>Ti<sub>3</sub>O<sub>12</sub> (and its other non-stoichiometric compositions). It belongs to ferroelectric species  $4/mmm \rightarrow m$  with the high Curie temperature ( $T_C = 675$  °C).
- tungsten-bronze structure — e.g., lead metaniobate PbNb<sub>2</sub>O<sub>6</sub>, is orthorhombic at room temperature ( $T_C = 570$  °C). It has very small planar coupling coefficient  $k_p$  and such resonators do not show coupling between planar and thickness vibration modes.

Research and technical application of lead-free piezoelectric ceramics systems is under intense research. Although very few lead-free ceramic systems are in the market, it could be anticipated as the future of piezoelectric ceramics manufacturing.

### 2.3 Example of Crystallographic Symmetry for Mechanically Textured Ceramics

Piezoelectric ceramics is prepared from ferroelectric ceramic grains of elongated shapes each with monoclinic symmetry (crystallographic group 2). Bar-shaped grains have monoclinic twofold symmetry axes oriented along the bar lengths, but other crystallographic axes are oriented arbitrarily with respect to grain. Ceramic grains are pressed uniaxially into green body with prevailing grains orientations in plane perpendicular to the pressing direction (i.e., longitudinal grain axes are perpendicular to the stress direction).

Electromechanical properties related to  $2_y$  crystallographic symmetry are listed in Appendix A. They are expressed in their crystallographic coordinate system. Each grain could be further arbitrarily rotated along its longitudinal y-axis by angle  $\psi$  and along perpendicular z-axis by angle  $\varphi$ . Coordinates of electromechanical tensors must be rotated by composite rotation from these two subsequent rotations as (see Nye 1985 for more detail)

$$\begin{aligned} \|a_{ij}\| &= \begin{pmatrix} \cos \psi & 0 & \sin \psi \\ 0 & 1 & 0 \\ -\sin \psi & 0 & \cos \psi \end{pmatrix} \cdot \begin{pmatrix} \cos \varphi & \sin \varphi & 0 \\ -\sin \varphi & \cos \varphi & 0 \\ 0 & 0 & 1 \end{pmatrix} \\ &= \begin{pmatrix} \cos \psi \cos \varphi & \sin \varphi & \sin \psi \cos \varphi \\ -\cos \psi \sin \varphi & \cos \varphi & -\sin \psi \sin \varphi \\ -\sin \psi & 0 & \cos \psi \end{pmatrix}. \end{aligned} \quad (2.1)$$

Components of permittivity (2nd rank tensor) are transformed as

$$\varepsilon'_{ij}(\varphi, \psi) = \sum_{l,m=1}^3 a_{il} a_{jm} \varepsilon_{lm}. \quad (2.2)$$

Permittivity components are therefore

$$\varepsilon'_{11}(\varphi, \psi) = [\varepsilon_{11} \cos^2 \psi + \varepsilon_{33} \sin^2 \psi + \varepsilon_{13} \sin(2\psi)] \cos^2 \varphi + \varepsilon_{22} \sin^2 \varphi, \quad (2.3a)$$

$$\varepsilon'_{12}(\varphi, \psi) = [-\varepsilon_{11} \cos^2 \psi - \varepsilon_{33} \sin^2 \psi + \varepsilon_{22} - \varepsilon_{13} \sin(2\psi)] \sin \varphi \cos \varphi, \quad (2.3b)$$

$$\varepsilon'_{13}(\varphi, \psi) = \frac{1}{2} \cos \varphi [2\varepsilon_{13} \cos(2\psi) + (\varepsilon_{33} - \varepsilon_{11}) \sin(2\psi)], \quad (2.3c)$$

$$\varepsilon'_{22}(\varphi, \psi) = [\varepsilon_{11} \cos^2 \psi + \varepsilon_{33} \sin^2 \psi + \varepsilon_{13} \sin(2\psi)] \sin^2 \varphi + \varepsilon_{22} \cos^2 \varphi, \quad (2.3d)$$

$$\varepsilon'_{23}(\varphi, \psi) = -\frac{1}{2} \sin \varphi [2\varepsilon_{13} \cos(2\psi) + (\varepsilon_{33} - \varepsilon_{11}) \sin(2\psi)], \quad (2.3e)$$

$$\varepsilon'_{33}(\varphi, \psi) = \varepsilon_{33} \cos^2 \psi + \sin \psi [\varepsilon_{11} \sin \psi - 2\varepsilon_{13} \cos \psi]. \quad (2.3f)$$

Components of piezoelectric tensor (3rd rank tensor) are transformed as

$$d'_{ijk}(\varphi, \psi) = \sum_{l,m,n=1}^3 a_{il} a_{jm} a_{kn} d_{lmn}. \quad (2.4)$$

Its components are then (taking into account matrix to tensor components transformation for piezoelectric charge tensor — see Appendix A)

$$d'_{11}(\varphi, \psi) = \sin \varphi \{ [(d_{16} + d_{21}) \cos^2 \psi + (d_{14} + d_{25} + d_{36}) \sin \psi \cos \psi + (d_{23} + d_{34}) \sin^2 \psi] \cos^2 \varphi + d_{22} \sin^2 \varphi \}, \quad (2.5a)$$

$$d'_{12}(\varphi, \psi) = \sin \varphi \{ [-d_{16} \cos^2 \psi - (d_{14} + d_{36}) \sin \psi \cos \psi - d_{34} \sin^2 \psi + d_{22}] \cos^2 \varphi + [d_{21} \cos^2 \psi + d_{25} \sin \psi \cos \psi + d_{23} \sin^2 \psi] \sin^2 \varphi \}, \quad (2.5b)$$

$$d'_{13}(\varphi, \psi) = \sin \varphi [d_{23} \cos^2 \psi - d_{25} \sin \psi \cos \psi + d_{21} \sin^2 \psi], \quad (2.5c)$$

$$d'_{14}(\varphi, \psi) = [d_{14} \cos^2 \psi - (d_{16} - d_{34}) \sin \psi \cos \psi - d_{36} \sin^2 \psi] \cos^2 \varphi - [d_{25} \cos(2\psi) + (d_{23} - d_{21}) \sin(2\psi)] \sin^2 \varphi, \quad (2.5d)$$

$$d'_{15}(\varphi, \psi) = \frac{1}{4} \sin(2\varphi) [d_{14} - d_{36} + (d_{14} + 2d_{25} + d_{36}) \cos(2\psi) + (-d_{16} - 2d_{21} + 2d_{23} + d_{34}) \sin(2\psi)], \quad (2.5e)$$

$$d'_{16}(\varphi, \psi) = \cos \varphi \{ [-2d_{21} \cos^2 \psi - 2d_{23} \sin^2 \psi + 2d_{22} - d_{25} \sin(2\psi)] \sin^2 \varphi + \cos(2\varphi) [d_{16} \cos^2 \psi + (d_{14} + d_{36}) \sin \psi \cos \psi + d_{34} \sin^2 \psi] \}, \quad (2.5f)$$

$$d'_{21}(\varphi, \psi) = \cos \varphi \{ [d_{21} \cos^2 \psi + d_{25} \sin \psi \cos \psi + d_{23} \sin^2 \psi] \cos^2 \varphi + [-d_{16} \cos^2 \psi - (d_{14} + d_{36}) \sin \psi \cos \psi - d_{34} \sin^2 \psi + d_{22}] \sin^2 \varphi \}, \quad (2.5g)$$

$$d'_{22}(\varphi, \psi) = \cos \varphi \{ d_{22} \cos^2 \varphi + [(d_{16} + d_{21}) \cos^2 \psi + (d_{14} + d_{25} + d_{36}) \sin \psi \cos \psi + (d_{23} + d_{34}) \sin^2 \psi] \sin^2 \varphi \}, \quad (2.5h)$$

$$d'_{23}(\varphi, \psi) = \cos \varphi [d_{23} \cos^2 \psi - d_{25} \sin \psi \cos \psi + d_{21} \sin^2 \psi], \quad (2.5i)$$

$$d'_{24}(\varphi, \psi) = -\frac{1}{4} \sin(2\varphi) [d_{14} - d_{36} + (d_{14} + 2d_{25} + d_{36}) \cos(2\psi) + (-d_{16} - 2d_{21} + 2d_{23} + d_{34}) \sin(2\psi)], \quad (2.5j)$$

$$d'_{25}(\varphi, \psi) = [d_{25} \cos(2\psi) + (d_{23} - d_{21}) \sin(2\psi)] \cos^2 \varphi + [-d_{14} \cos^2 \psi + (d_{16} - d_{34}) \sin \psi \cos \psi + d_{36} \sin^2 \psi] \sin^2 \varphi, \quad (2.5k)$$

$$d'_{26}(\varphi, \psi) = \sin \varphi \{ [-2d_{21} \cos^2 \psi - 2d_{23} \sin^2 \psi + 2d_{22} - d_{25} \sin(2\psi)] \cos^2 \varphi - \cos(2\varphi) [d_{16} \cos^2 \psi + (d_{14} + d_{36}) \sin \psi \cos \psi + d_{34} \sin^2 \psi] \}, \quad (2.5l)$$

$$d'_{31}(\varphi, \psi) = \sin \varphi \cos \varphi [d_{36} \cos^2 \psi - (d_{16} - d_{34}) \sin \psi \cos \psi - d_{14} \sin^2 \psi], \quad (2.5m)$$

$$d'_{32}(\varphi, \psi) = \sin \varphi \cos \varphi [-d_{36} \cos^2 \psi + (d_{16} - d_{34}) \sin \psi \cos \psi + d_{14} \sin^2 \psi], \quad (2.5n)$$

$$d'_{33}(\varphi, \psi) = 0, \quad (2.5o)$$

$$d'_{34}(\varphi, \psi) = \cos \varphi [d_{34} \cos^2 \psi - (d_{14} + d_{36}) \sin \psi \cos \psi + d_{16} \sin^2 \psi], \quad (2.5p)$$

$$d'_{35}(\varphi, \psi) = \sin \varphi [d_{34} \cos^2 \psi - (d_{14} + d_{36}) \sin \psi \cos \psi + d_{16} \sin^2 \psi], \quad (2.5q)$$

$$d'_{36}(\varphi, \psi) = \frac{1}{2} \cos(2\varphi) [-d_{14} + d_{36} + (d_{14} + d_{36}) \cos(2\psi) + (d_{34} - d_{16}) \sin(2\psi)]. \quad (2.5r)$$

Components of elastic modulus tensor (4th rank tensor) are transformed as

$$c'_{ijkl}(\varphi, \psi) = \sum_{m,n,p,q=1}^3 a_{im} a_{jn} a_{kp} a_{lq} c_{mnpq}. \quad (2.6)$$

Its components are then (taking into account matrix to tensor components transformation for elastic modulus tensor — see Appendix A)

$$\begin{aligned}
c'_{11}(\varphi, \psi) = & [c_{11} \cos^4 \psi + 4c_{15} \sin \psi \cos^3 \psi + 2(c_{13} + 2c_{55}) \sin^2 \psi \cos^2 \psi \\
& + 4c_{35} \sin^3 \psi \cos \psi + c_{33} \sin^4 \psi] \cos^4 \varphi \\
& + [c_{12} + c_{23} + 2c_{44} + 2c_{66} + (c_{12} - c_{23} - 2c_{44} + 2c_{66}) \cos(2\psi) \\
& + 2(c_{25} + 2c_{46}) \sin(2\psi)] \sin^2 \varphi \cos^2 \varphi + c_{22} \sin^4 \varphi,
\end{aligned} \tag{2.7a}$$

$$\begin{aligned}
c'_{12}(\varphi, \psi) = & [c_{12} \cos^2 \psi + c_{23} \sin^2 \psi + c_{25} \sin(2\psi)] \cos^4 \varphi \\
& + [c_{11} \cos^4 \psi + 4c_{15} \sin \psi \cos^3 \psi + (2c_{13} \sin^2 \psi + 4c_{55} \sin^2 \psi - 4c_{66}) \cos^2 \psi \\
& + 4c_{35} \sin^3 \psi \cos \psi + c_{33} \sin^4 \psi - 4c_{44} \sin^2 \psi + c_{22} - 4c_{46} \sin(2\psi)] \sin^2 \varphi \cos^2 \varphi \\
& + [c_{12} \cos^2 \psi + c_{23} \sin^2 \psi + c_{25} \sin(2\psi)] \sin^4 \varphi,
\end{aligned} \tag{2.7b}$$

$$\begin{aligned}
c'_{13}(\varphi, \psi) = & [c_{23} \cos^2 \psi + c_{12} \sin^2 \psi - c_{25} \sin(2\psi)] \sin^2 \varphi \\
& - \frac{1}{8} [-c_{11} - 6c_{13} - c_{33} + 4c_{55} + (c_{11} - 2c_{13} + c_{33} - 4c_{55}) \cos(4\psi) \\
& + 4(c_{15} - c_{35}) \sin(4\psi)] \cos^2 \varphi,
\end{aligned} \tag{2.7c}$$

$$\begin{aligned}
c'_{14}(\varphi, \psi) = & \sin \varphi \left\{ -\frac{1}{8} [4(c_{15} + c_{35} - 4c_{46}) \cos(2\psi) + 4(c_{15} - c_{35}) \cos(4\psi) \right. \\
& + 2(-c_{11} + c_{33} - 4c_{44} + 4c_{66}) \sin(2\psi) + (-c_{11} + 2c_{13} - c_{33} + 4c_{55}) \sin(4\psi)] \cos^2 \varphi \\
& \left. - [c_{25} \cos(2\psi) + (c_{23} - c_{12}) \sin \psi \cos \psi] \sin^2 \varphi \right\},
\end{aligned} \tag{2.7d}$$

$$\begin{aligned}
c'_{15}(\varphi, \psi) = & \frac{1}{8} \cos \varphi \{ [4(c_{15} + c_{35}) \cos(2\psi) + 4(c_{15} - c_{35}) \cos(4\psi) + 2(-c_{11} + c_{33}) \sin(2\psi) \\
& + (-c_{11} + 2c_{13} - c_{33} + 4c_{55}) \sin(4\psi)] \cos^2 \varphi \\
& + 4[2(c_{25} + 2c_{46}) \cos(2\psi) + (-c_{12} + c_{23} + 2c_{44} - 2c_{66}) \sin(2\psi)] \sin^2 \varphi \},
\end{aligned} \tag{2.7e}$$

$$\begin{aligned}
c'_{16}(\varphi, \psi) = & -\sin \varphi \cos \varphi \{ [c_{11} \cos^4 \psi + 4c_{15} \sin \psi \cos^3 \psi + 2(c_{13} + 2c_{55}) \sin^2 \psi \cos^2 \psi \\
& - (c_{12} + 2c_{66}) \cos^2 \psi + 4c_{35} \sin^3 \psi \cos \psi + c_{33} \sin^4 \psi - (c_{23} + 2c_{44}) \sin^2 \psi \\
& - (c_{25} + 2c_{46}) \sin(2\psi)] \cos^2 \varphi + [(c_{12} + 2c_{66}) \cos^2 \psi + (c_{23} + 2c_{44}) \sin^2 \psi \\
& - c_{22} + (c_{25} + 2c_{46}) \sin(2\psi)] \sin^2 \varphi \},
\end{aligned} \tag{2.7f}$$

$$\begin{aligned}
c'_{22}(\varphi, \psi) = & [c_{12} + c_{23} + 2c_{44} + 2c_{66} + (c_{12} - c_{23} - 2c_{44} + 2c_{66}) \cos(2\psi) \\
& + 2(c_{25} + 2c_{46}) \sin(2\psi)] \sin^2 \varphi \cos^2 \varphi + [c_{11} \cos^4 \psi + 4c_{15} \sin \psi \cos^3 \psi \\
& + 2(c_{13} + 2c_{55}) \sin^2 \psi \cos^2 \psi + 4c_{35} \sin^3 \psi \cos \psi + c_{33} \sin^4 \psi] \sin^4 \varphi + c_{22} \cos^4 \varphi,
\end{aligned} \tag{2.7g}$$

$$\begin{aligned}
c'_{23}(\varphi, \psi) = & [c_{23} \cos^2 \psi + c_{12} \sin^2 \psi - c_{25} \sin(2\psi)] \cos^2 \varphi \\
& - \frac{1}{8} [-c_{11} - 6c_{13} - c_{33} + 4c_{55} + (c_{11} - 2c_{13} + c_{33} - 4c_{55}) \cos(4\psi) \\
& + 4(c_{15} - c_{35}) \sin(4\psi)] \sin^2 \varphi,
\end{aligned} \tag{2.7h}$$

$$\begin{aligned}
c'_{24}(\varphi, \psi) = & -\frac{1}{8} \sin \varphi \{ 4[2(c_{25} + 2c_{46}) \cos(2\psi) + (-c_{12} + c_{23} + 2c_{44} - 2c_{66}) \sin(2\psi)] \cos^2 \varphi \\
& + [4(c_{15} + c_{35}) \cos(2\psi) + 4(c_{15} - c_{35}) \cos(4\psi) + 2(-c_{11} + c_{33}) \sin(2\psi) \\
& + (-c_{11} + 2c_{13} - c_{33} + 4c_{55}) \sin(4\psi)] \sin^2 \varphi \}, \tag{2.7i}
\end{aligned}$$

$$\begin{aligned}
c'_{25}(\varphi, \psi) = & \cos \varphi \{ [c_{25} \cos(2\psi) + (c_{23} - c_{12}) \sin \psi \cos \psi] \cos^2 \varphi \\
& + \frac{1}{8} [4(c_{15} + c_{35} - 4c_{46}) \cos(2\psi) + 4(c_{15} - c_{35}) \cos(4\psi) \\
& + 2(-c_{11} + c_{33} - 4c_{44} + 4c_{66}) \sin(2\psi) \\
& + (-c_{11} + 2c_{13} - c_{33} + 4c_{55}) \sin(4\psi)] \sin^2 \varphi \}, \tag{2.7j}
\end{aligned}$$

$$\begin{aligned}
c'_{26}(\varphi, \psi) = & \sin \varphi \cos \varphi \{ [- (c_{12} + 2c_{66}) \cos^2 \psi - (c_{23} + 2c_{44}) \sin^2 \psi + c_{22} \\
& - (c_{25} + 2c_{46}) \sin(2\psi)] \cos^2 \varphi + [-c_{11} \cos^4 \psi - 4c_{15} \sin \psi \cos^3 \psi \\
& - 2(c_{13} + 2c_{55}) \sin^2 \psi \cos^2 \psi + (c_{12} + 2c_{66}) \cos^2 \psi - 4c_{35} \sin^3 \psi \cos \psi \\
& - c_{33} \sin^4 \psi + (c_{23} + 2c_{44}) \sin^2 \psi + (c_{25} + 2c_{46}) \sin(2\psi)] \sin^2 \varphi \}, \tag{2.7k}
\end{aligned}$$

$$\begin{aligned}
c'_{33}(\varphi, \psi) = & c_{33} \cos^4 \psi - 4c_{35} \sin \psi \cos^3 \psi + 2(c_{13} + 2c_{55}) \sin^2 \psi \cos^2 \psi \\
& - 4c_{15} \sin^3 \psi \cos \psi + c_{11} \sin^4 \psi, \tag{2.7l}
\end{aligned}$$

$$\begin{aligned}
c'_{34}(\varphi, \psi) = & -\frac{1}{8} \sin \varphi \{ -4(c_{15} - c_{35}) \cos(4\psi) + 2(c_{33} - c_{11}) \sin(2\psi) + 2 \cos(2\psi) \\
& [2(c_{15} + c_{35}) + (c_{11} - 2c_{13} + c_{33} - 4c_{55}) \sin(2\psi)] \}, \tag{2.7m}
\end{aligned}$$

$$\begin{aligned}
c'_{35}(\varphi, \psi) = & \frac{1}{8} \cos \varphi \{ -4(c_{15} - c_{35}) \cos(4\psi) + 2(c_{33} - c_{11}) \sin(2\psi) + 2 \cos(2\psi) \\
& [2(c_{15} + c_{35}) + (c_{11} - 2c_{13} + c_{33} - 4c_{55}) \sin(2\psi)] \}, \tag{2.7n}
\end{aligned}$$

$$\begin{aligned}
c'_{36}(\varphi, \psi) = & \frac{1}{16} \sin(2\varphi) [-c_{11} + 4c_{12} - 6c_{13} + 4c_{23} - c_{33} + 4c_{55} - 4(c_{12} - c_{23}) \cos(2\psi) \\
& + (c_{11} - 2c_{13} + c_{33} - 4c_{55}) \cos(4\psi) - 8c_{25} \sin(2\psi) + 4(c_{15} - c_{35}) \sin(4\psi)], \tag{2.7o}
\end{aligned}$$

$$\begin{aligned}
c'_{44}(\varphi, \psi) = & \cos^2 \varphi [c_{44} \cos^2 \psi + c_{66} \sin^2 \psi - c_{44} \sin(2\psi)] \\
& - \frac{1}{8} \sin^2 \varphi [-c_{11} + 2c_{13} - c_{33} - 4c_{55} + (c_{11} - 2c_{13} + c_{33} - 4c_{55}) \cos(4\psi) \\
& + 4(c_{15} - c_{35}) \sin(4\psi)], \tag{2.7p}
\end{aligned}$$

$$\begin{aligned}
c'_{45}(\varphi, \psi) = & \frac{1}{16} \sin(2\varphi) [-c_{11} + 2c_{13} - c_{33} + 4c_{44} - 4c_{55} + 4c_{66} + 4(c_{44} - c_{66}) \cos(2\psi) \\
& + (c_{11} - 2c_{13} + c_{33} - 4c_{55}) \cos(4\psi) - 8c_{46} \sin(2\psi) + 4(c_{15} - c_{35}) \sin(4\psi)], \tag{2.7q}
\end{aligned}$$

$$\begin{aligned}
c'_{46}(\varphi, \psi) = & \frac{1}{8} \cos \varphi \{ [4(c_{15} - 2c_{25} + c_{35}) \cos(2\psi) + 4(c_{15} - c_{35}) \cos(4\psi) \\
& + 2(-c_{11} + 2c_{12} - 2c_{23} + c_{33}) \sin(2\psi) + (-c_{11} + 2c_{13} - c_{33} + 4c_{55}) \sin(4\psi)] \sin^2 \varphi \\
& + 4 \cos(2\varphi) [2c_{46} \cos(2\psi) + (c_{44} - c_{66}) \sin(2\psi)] \},
\end{aligned} \tag{2.7r}$$

$$\begin{aligned}
c'_{55}(\varphi, \psi) = & \sin^2 \varphi [c_{44} \cos^2 \psi + c_{66} \sin^2 \psi - c_{44} \sin(2\psi)] \\
& - \frac{1}{8} \cos^2 \varphi [-c_{11} + 2c_{13} - c_{33} - 4c_{55} + (c_{11} - 2c_{13} + c_{33} - 4c_{55}) \cos(4\psi) \\
& + 4(c_{15} - c_{35}) \sin(4\psi)],
\end{aligned} \tag{2.7s}$$

$$\begin{aligned}
c'_{56}(\varphi, \psi) = & \frac{1}{8} \sin \varphi \{ [-4(c_{15} - 2c_{25} + c_{35}) \cos(2\psi) - 4(c_{15} - c_{35}) \cos(4\psi) \\
& - 2(-c_{11} + 2c_{12} - 2c_{23} + c_{33}) \sin(2\psi) - (-c_{11} + 2c_{13} - c_{33} + 4c_{55}) \sin(4\psi)] \\
& \cos^2 \varphi + 4 \cos(2\varphi) [2c_{46} \cos(2\psi) + (c_{44} - c_{66}) \sin(2\psi)] \},
\end{aligned} \tag{2.7t}$$

$$\begin{aligned}
c'_{66}(\varphi, \psi) = & (\sin^4 \varphi + \cos^4 \varphi) [c_{66} \cos^2 \psi + c_{44} \sin^2 \psi + c_{46} \sin(2\psi)] \\
& + \sin^2 \varphi \cos^2 \varphi [c_{11} \cos^4 \psi + 4c_{15} \sin \psi \cos^3 \psi + 2(c_{13} + 2c_{55}) \sin^2 \psi \cos^2 \psi \\
& - 2(c_{12} + c_{66}) \cos^2 \psi + 4c_{35} \sin^3 \psi \cos \psi + c_{33} \sin^4 \psi - 2(c_{23} + c_{44}) \sin^2 \psi \\
& + c_{22} - 2(c_{25} + c_{46}) \sin(2\psi)].
\end{aligned} \tag{2.7u}$$

Averaging of electromechanical properties over rotation angles  $\varphi, \psi$

$$\varepsilon_{ij}^{\text{eff}} = \frac{1}{(2\pi)^2} \int_0^{2\pi} \int_0^{2\pi} \varepsilon'_{ij}(\varphi, \psi) d\varphi d\psi, \tag{2.8a}$$

$$d_{ix}^{\text{eff}} = \frac{1}{(2\pi)^2} \int_0^{2\pi} \int_0^{2\pi} d'_{ix}(\varphi, \psi) d\varphi d\psi, \tag{2.8b}$$

$$c_{\alpha\beta}^{\text{eff}} = \frac{1}{(2\pi)^2} \int_0^{2\pi} \int_0^{2\pi} c'_{\alpha\beta}(\varphi, \psi) d\varphi d\psi \tag{2.8c}$$

results in the following non-zero coefficients

$$c_{11}^{\text{eff}} = c_{22}^{\text{eff}} = \frac{1}{8} (c_{12} + c_{23} + 2c_{44} + 2c_{66} + 3c_{22}) + \frac{3}{64} (3c_{11} + 2c_{13} + 4c_{55} + 3c_{33}), \tag{2.9a}$$

$$c_{12}^{\text{eff}} = \frac{1}{8} (3c_{12} + 3c_{23} - 2c_{44} - 2c_{66} + c_{22}) + \frac{1}{64} (3c_{11} + 2c_{13} + 4c_{55} + 3c_{33}), \tag{2.9b}$$

$$c_{13}^{\text{eff}} = c_{23}^{\text{eff}} = \frac{1}{4}(c_{12} + c_{23}) + \frac{1}{16}(c_{11} + 6c_{13} - 4c_{55} + c_{33}), \quad (2.9c)$$

$$c_{33}^{\text{eff}} = \frac{1}{8}(3c_{33} + 2c_{13} + 4c_{55} + 3c_{11}), \quad (2.9d)$$

$$c_{44}^{\text{eff}} = c_{55}^{\text{eff}} = \frac{1}{4}(c_{44} + c_{66}) + \frac{1}{16}(c_{11} - 2c_{13} + 4c_{55} + c_{33}), \quad (2.9e)$$

$$\begin{aligned} c_{66}^{\text{eff}} &= \frac{1}{2}(c_{11}^{\text{eff}} - c_{12}^{\text{eff}}) \\ &= \frac{1}{8}(-c_{12} - c_{23} + 2c_{44} + 2c_{66} + c_{22}) + \frac{1}{64}(3c_{11} + 2c_{13} + 4c_{55} + 3c_{33}), \end{aligned} \quad (2.9f)$$

$$d_{14}^{\text{eff}} = -d_{25}^{\text{eff}} = \frac{1}{4}(d_{14} - d_{36}), \quad (2.9g)$$

$$\varepsilon_{11}^{\text{eff}} = \varepsilon_{22}^{\text{eff}} = \frac{1}{4}(\varepsilon_{11} + 2\varepsilon_{22} + \varepsilon_{33}), \quad (2.9h)$$

$$\varepsilon_{33}^{\text{eff}} = \frac{1}{2}(\varepsilon_{11} + \varepsilon_{33}). \quad (2.9i)$$

Effective symmetry corresponds to the limiting symmetry — Curie group  $\infty 2$  (see Appendix A).

## References

- Berlincourt D (1981) Piezoelectric ceramics: characteristics and applications. *J Acoust Soc Am* 70:1586–1595
- Bhalla AS, Guo R, Roy R (2000) The perovskite structure — a review of its role in ceramic science and technology. *Mat Res Innovat* 4:3–26
- Buchanan RC (ed) (1986) *Ceramic materials for electronics — processing, properties and applications*. Marcel Dekker, New York
- Cross LE (1996) Ferroelectric materials for electromechanical transducer applications. *Mat Chem Phys* 43:108–115
- Heywang W, Lubitz K, Wersing W (eds) (2008) *Piezoelectricity, evolution and future of a technology*. Springer, Berlin
- Jaffe B, Cook WR, Jaffe H (1971) *Piezoelectric ceramics*. Academic Press, London
- Levinson LM (1988) *Electronic ceramics — properties, devices and applications*. Marcel Dekker, New York
- Messing GL, Trolier-McKinstry S, Sabolsky EM, Duran C, Kwon S, Brahmaroutu B, Park P, Yilmaz H, Rehrig PW, Eitel KB, Suvaci E, Seabaugh M, Oh KS (2004) Templated grain growth of textured piezoelectric ceramics. *Crit Rev Solid State Mater Sci* 29:45–96
- Nowotny J (ed) (1992) *Electronic ceramic materials*. *Key Eng Mater* 66–67



- Nye JF (1985) Physical properties of crystals, Their representation by tensors and matrices. Clarendon Press, Oxford
- Priya S, Nahm S (eds) (2012) Lead-free piezoelectrics. Springer, Berlin
- Redin RD, Marks GW, Antoniak CE (1963) Symmetry limitations to polarization of polycrystalline ferroelectrics. *J Appl Phys* 34:600–610
- Rödel J, Webber KG, Dittmer R, Jo Wook, Kimura M, Damjanovic D (2015) Transferring lead-free piezoelectric ceramics into application. *J Eur Ceram Soc* 35:1659–1681
- Saito Y, Takao H, Tani T, Nonoyama T, Takatori K, Homma T, Nagaya T, Nakamura M (2004) Lead-free piezoceramics. *Nature* 432:84–87
- Setter N, Colla EL (1993) Ferroelectric ceramics: tutorial reviews, theory, processing, and applications. Birkhäuser Verlag
- Shrout TR, Zhang SJ (2007) Lead-free piezoelectric ceramics: alternatives for PZT? *J Electroceram* 19:113–126
- Tichý J, Erhart J, Kittinger E, Přivratská J (2010) Fundamentals of piezoelectric sensorics: mechanical, dielectric, and thermodynamical properties of piezoelectric materials. Springer, Heidelberg, Berlin
- Yang SL, Chen SM, Tsai CC, Hong CS, Chu SY (2013) Fabrication of high-power piezoelectric transformers using lead-free ceramics for application in electronic ballasts. *IEEE Trans UFFC* 60(2):408–413

Piezoelectric Ceramic Resonators

Erhart, J.; PŰlpán, P.; Pustka, M.

2017, XVII, 251 p. 111 illus., 43 illus. in color.,

Hardcover

ISBN: 978-3-319-42480-4